



ARTICLE

# Effect of Polyisobutylene Succinimide on the Physical Stability of an Environmentally Friendly Pesticide Oil Dispersion Suspension

Liyang Wang\*, Junzhi Liu, Chong Gao and Xinxin Yan

Institute of Functional Molecules, Shenyang University of Chemical Technology, Shenyang, 110142, China

\*Corresponding Author: Liyang Wang. Email: wangliyang401@163.com

Received: 20 July 2022 Accepted: 01 September 2022

## ABSTRACT

Oil dispersible suspension concentrates are safe, green, and environmentally friendly formulations. Problems such as layering, pasting, and bottoming are frequently encountered during the production, storage, and transportation process. Polyisobutylene succinimide functions as a dispersant and exhibits great potential to improve the physical stability of the oil dispersible suspension concentrate. From a microscopic perspective, the sorption characteristics of the polyisobutylene succinimide dispersant T151 on penoxsulam particle surfaces were comprehensively evaluated with XPS, FTIR, and SEM. The T151 adsorption procedure complied with a pseudo-second-order kinetic adsorption model, and it was a kind of physical sorption with an  $E_a$  of  $22.57 \text{ kJ}\cdot\text{mol}^{-1}$ . The T151 sorption model was consistent with the Langmuir isotherm. The adsorption process was spontaneous and followed by an entropy increase. The  $\Delta H^\theta$  of dispersant T151 on the surface of penoxsulam particles was  $31.59 \text{ kJ}\cdot\text{mol}^{-1}$ . The adsorption procedure was endothermic, and the primary force was hydrogen bonding. The XPS results showed that the F and S electronic peaks at the penoxsulam interface decreased, and that the C electronic peak increased significantly after the adsorption of dispersant T151, indicating the adsorption on the surface of penoxsulam particles. The results of this study provide a vital theoretical basis for the application of polyisobutylene succinimide dispersants in oil dispersible suspension systems.

## KEYWORDS

Polyisobutylene succinimide; oil dispersion suspension; penoxsulam; physical stability

## 1 Introduction

As a safe, green, and environmentally friendly formulation, oil-dispersible suspension concentrates have become an area of particular interest in the development of pesticide formulations over the last 10 years [1,2]. In an oil dispersion suspension concentrate, the various additive and active ingredient solid particles are dispersed in a non-aqueous medium-based environmentally friendly. This is done after wet grinding to form a stable suspension system, which is diluted with water before use. In the agriculture industry, oil dispersion suspension concentrates have the following advantages: (1) no dust during production and application, which improves worker safety; (2) no flammable and explosive solvents, making production, use, and storage relatively safe; (3) use of oil as the dispersion medium, which is less toxic and thus more environmentally friendly; (4) good wetting, spreading, permeability, and strong resistance to rain erosion; and (5) the synergistic effect of the oil dispersion medium improves the control effect. Therefore, the oil



dispersion suspension concentrate meets the requirements of green agricultural development and has numerous market prospects.

However, in the production, storage, and transportation phases, oil-dispersible suspension concentrates are prone to quality issues, such as delamination, pasting, and bottoming, which limits their application [3]. This is because oil dispersible (OD) is a nonhomogeneous solid–liquid dispersion system that exhibits significant thermodynamic instability. It is usually necessary to add a dispersant to maintain physical stability [4,5]. However, commonly used dispersants in pesticide processing, such as naphthalene sulfonates and polycarboxylates, are primarily used in aqueous media and are unsuitable for oil-dispersible suspension concentrates [6]. Therefore, dispersant excavation for a non-aqueous medium and enhancement of the physical stability of the OD are required in pesticide processing.

Polyisobutylene succinimide is a dispersant that performs favorably, has good dispersibility in non-aqueous media, and is widely used in the lubricating oil industry [7,8]. It can disperse soot powder and carbon nanotubes better in a hydrocarbon solution and reduce the viscosity of the system [9–11]. Zhang et al. [12] discovered the effect of polyisobutylene succinimide on the colloidal stability of clay particles in nonpolar media. Polyisobutylene succinimide has great potential as a dispersant to improve the physical stability of OD, particularly in the pesticide industry. However, the application of polyisobutylene succinimide in pesticide formulations has not yet been reported.

The effect of the dispersants is exerted by their adsorption on the pesticide particle surfaces and the adsorption stability is maintained by the steric hindrance and/or electrostatic repulsion effects to prevent the aggregation of pesticide particles. Therefore, it is particularly important to study the sorption behavior of dispersants on the pesticide granule faces for their practical application and the development of pesticide formulations. Several domestic and foreign researchers have focused on this topic. Xu et al. [13,14] reported on the spectroscopic characteristics of the sorption of polycarboxylate copolymer dispersants on the surface of atrazine granules. Zhang et al. [15] studied the adsorption characteristics of styrene-acrylic acid and naphthalene sulfonate-formaldehyde copolymers with different molecular weights on the surface of hexaflumuron particles. Pang et al. [16] determined the adsorption properties of different sodium lignosulfonate dispersants on the surface of dimethomorph particles. Ma et al. [17] found the sorption properties of a comb-shaped polycarboxylic acid superplasticizer copolymer on fipronil granule faces. Hao et al. [18] discussed the sorption characteristics of several anionic dispersants on the faces of imidacloprid granules using the oscillating adsorption method. However, the adsorption characteristics of these different dispersants on the pesticide particle surfaces were evaluated in a system using water as the medium. There are insufficient systematic and in-depth studies on the adsorption characteristics of dispersants on the surfaces of pesticide particles in non-aqueous media.

Penoxsulam, developed by Dow AgroSciences, is a triazolopyrimidine sulfonamide herbicide used in paddy fields. It is an acetolactate synthase (ALS) inhibitor that can be used to control barnyard grass, broadleaf weeds, sedge, and some aquatic weeds before and after germination [19]. A 25 g/L penoxsulam oil dispersible suspension concentrate has been registered and shows great market potential [20,21]. In this study, the effect of polyisobutylene succinimide on the stability of a penoxsulam oil dispersible suspension concentrate was investigated using multiple light scattering technologies [22]. The adsorption thermodynamics, kinetics, and force, and thickness of the polyisobutylene succinimide adsorption layer on penoxsulam particle surfaces in non-aqueous media were examined using XPS, FTIR, and SEM [23,24]. Furthermore, the underlying stability mechanism is discussed, and a theoretical basis for the application of polyisobutylene succinimide in oil-dispersible suspension concentrates is provided.

## 2 Materials and Methods

### 2.1 Materials

Penoxsulam (98%) was obtained from Zhejiang Tianyi Agrochemical Co. Ltd., Zhejiang, China. The molecular structure of penoxsulam is shown in Fig. 1A. Polyisobutylene succinimide (T151, MW = 7004, tested by GPC) was provided by Jianqiao Chemical Co., Ltd., Jiangsu, China. The molecular structure of T151 is shown in Fig. 1B. Analytical grade N-octane was purchased from Aladdin Reagent Co., Ltd., Shanghai, China.

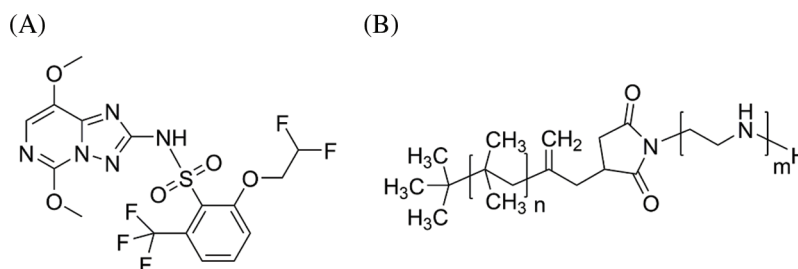


**Figure 1:** Chemical structures of penoxsulam (A) and T151 (B)

### 2.2 Dispersion Stability Analysis

Wet pulverization equipment was employed to prepare the penoxsulam oil dispersible suspension concentrate. We weighed a certain quantity of penoxsulam (5%) and T151 (4%), composed of up to 100% with methyl oleate, mixed them evenly, and cut them with a high shear emulsifier for 1–2 min. The mixture was then added to a sand mill and sanded for 3 h, and the sample was obtained after filtration.

The prepared penoxsulam oil dispersible suspension concentrate (20 mL) was added to the sample vial and scanned it hourly at 25°C for 48 h using a multiple light scattering instrument (Turbiscan Tower, Formulation, France) [25,26]. A stability index (TSI) was used to measure the stability of each sample.

### 2.3 Adsorption Thermodynamic

The T151 adsorption isotherm on the surface of the penoxsulam granules was determined using the oscillation adsorption method [27–29]. Penoxsulam powder and T151 n-octane solution were weighed and placed in a 100 mL triangular flask. Once sealed, the samples were shaken at three different temperatures for a given time. The supernatant was filtered and diluted, and its mass concentration was measured using a UV-1800 (Shimadzu, Japan) once the adsorption balance was achieved. A blank test was performed to remove the penoxsulam disturbance in n-octane during UV absorption. The adsorption capacity was calculated using Eq. (1):

$$Q_t = (C_0 - C_t + C_b)V/m, \quad (1)$$

where  $Q_t$  ( $\text{mg}\cdot\text{g}^{-1}$ ) is the mass of T151 adsorbed per gram of penoxsulam;  $C_0$  ( $\text{mg}\cdot\text{L}^{-1}$ ) is the concentration of the T151 solution;  $C_t$  ( $\text{mg}\cdot\text{L}^{-1}$ ) is the concentration of the solution after the sorption balance;  $C_b$  ( $\text{mg}\cdot\text{L}^{-1}$ ) is the concentration of the blank sample;  $V$  (L) is the volume of the T151 solution; and  $m$  (g) is the mass of penoxsulam.

The Langmuir and Freundlich isotherm equations are widely used to discuss adsorption procedures using experimental data [30–33].

The general form of the Langmuir equation is given by Eq. (2):

$$C_e/Q_t = 1/aQ_e + C_e/Q_e, \quad (2)$$

The Freundlich equation is given by Eq. (3) [34–36]:

$$\ln Q_t = (1/n)\ln C_e + \ln K_f, \quad (3)$$

where  $Q_t$  ( $\text{mg}\cdot\text{g}^{-1}$ ) is the apparent adsorption quantity;  $Q_e$  ( $\text{mg}\cdot\text{g}^{-1}$ ) is the saturated adsorption quantity;  $a$  ( $\text{L}\cdot\text{g}^{-1}$ ) is the Langmuir adsorption constant;  $C_e$  ( $\text{mg}\cdot\text{L}^{-1}$ ) is the concentration at adsorption equilibrium; and  $K_f$  and  $n$  are the adsorption constants.

Adsorption thermodynamics were evaluated by calculating the Gibbs free energy ( $\Delta G^\theta$ ), entropy change ( $\Delta S^\theta$ ), and enthalpy change ( $\Delta H^\theta$ ) [37]. The three thermodynamic parameters and the adsorption equilibrium constants were calculated using Eqs. (4)–(7):

$$K = M_w C_B b, \quad (4)$$

$$\Delta G^\theta = \Delta H^\theta - T\Delta S^\theta = -RT\ln K, \quad (5)$$

$$\ln K = (\Delta S^\theta/R) - (\Delta H^\theta/RT), \quad (6)$$

$$\Delta S^\theta = (\Delta H^\theta - \Delta G^\theta)/T, \quad (7)$$

## 2.4 Adsorption Kinetics

The T151 adsorption kinetic curve on the surface of the penoxsulam particles was determined using the oscillatory adsorption method [38–40]. Penoxsulam powder and T151 n-octane solution were weighed and placed in a 100 mL triangular flask. After sealing, the samples were shaken at three different temperatures for a given time. A blank test was conducted simultaneously to remove the UV absorption disturbance by penoxsulam in n-octane. The supernatant was collected periodically to measure its concentration using the method described in Section 2.3.

The adsorption kinetic constants were evaluated by fitting the pseudo-first-order kinetic model Eq. (8) and the pseudo-second-order kinetic model in Eq. (9) [41]:

$$\ln(Q_e - Q_t) = \ln Q_e - k_1 t, \quad (8)$$

$$t/Q_t = 1/k_2 Q_e^2 + t/Q_e, \quad (9)$$

where  $Q_t$  ( $\text{mg}\cdot\text{g}^{-1}$ ) is the apparent adsorption quantity;  $Q_e$  ( $\text{mg}\cdot\text{g}^{-1}$ ) is the saturated adsorption quantity;  $k_1$  ( $\text{min}^{-1}$ ) and  $k_2$  ( $\text{g}\cdot\text{mg}^{-1}\cdot\text{min}^{-1}$ ) are the adsorption rate constants of the pseudo-first-order and pseudo-second-order kinetic equations, respectively; and  $t$  (min) is the adsorption time.

The adsorption rate constant ( $k$ ) was calculated using Eq. (10):

$$\ln k = \ln z - E_a/RT, \quad (10)$$

where  $k$  is the adsorption rate constant;  $E_a$  ( $\text{kJ}\cdot\text{mol}^{-1}$ ) is the apparent activation energy;  $R$  ( $8.314 \text{ J}\cdot\text{K}^{-1}\cdot\text{mol}^{-1}$ ) is the gas constant;  $T$  (K) is the temperature; and  $z$  is the Arrhenius factor [42].

## 2.5 XPS Analysis

The penoxsulam powder and T151 n-octane solution put in a 100 mL triangular flask and oscillated for 5 h at 293.15, 303.15, and 313.15 K [43–45]. After oscillation, the suspension was centrifuged, washed, and dried under a vacuum. The obtained powder was analyzed using XPS (Axis Ultra, Kratos, UK).

## 2.6 FTIR Analysis

The penoxsulam suspension was oscillated for a while at 293.15 K and then centrifuged. The filter cake was dried under vacuum and then pressed with KBr for FTIR (Tracer-IR 100, Shimadzu, Japan) scanning.

## 2.7 Microscopic Analysis

SEM (S-4800, Hitachi, Japan) was used to observe the morphology of the samples. The dried powder sample was sputtered with a layer of gold prior to imaging.

# 3 Results and Discussion

## 3.1 Dispersion Stability

The multilight scattering technique can report the change in grain diameter and concentration of the dispersion system from the curves of backscattered and transmitted light over time. The stability of the dispersion system was analyzed using the TSI value. In general, the smaller the TSI value, the better the stability of the dispersion system.

The time-dependent transmitted and backscattered light spectra of the penoxsulam oil dispersible suspension concentrate with and without dispersant T151 were investigated. There was no transmitted light at the top of the sample with T151 (Fig. 2A), whereas there was transmitted light without T151 (Fig. 2B), indicating that the sample with T151 was not delaminated, while the sample without T151 was delaminated. The total TSI with T151 was 1.6 and the total TSI without T151 was 39.0 (Table 1). Therefore, dispersant T151 is helpful in eliminating the formulation delamination phenomenon and enhancing the stability of the penoxsulam oil dispersible suspension concentrate.

## 3.2 Adsorption Thermodynamics

### 3.2.1 Adsorption Isotherm

From a thermodynamic perspective, adsorption is a surface phenomenon involving adsorbate aggregation from the solvent on the face of the adsorbent. Sorption equilibria are controlled by several factors, including the properties of the adsorbent and adsorbate, and the temperature [18]. Herein, the dispersant was the adsorbate, and penoxsulam was used as the adsorbent. The sorption isotherms of T151 on the surface of the penoxsulam particles were measured at 293.15, 303.15, and 313.15 K, as shown in Fig. 3.

At the same temperature, the quantity of T151 adsorbed on the surface of penoxsulam increased with increasing equilibrium concentration. The adsorption capacity increased rapidly when the equilibrium concentration was low; the adsorption capacity decreased slowly and reached saturation when the balance concentration reached a certain value. The T151 adsorption ability on the penoxsulam surface increased with increasing temperature, and it was easier to achieve saturated adsorption at a higher temperature (Fig. 3).

### 3.2.2 Adsorption Models

The Langmuir and Freundlich sorption equations were applied to fit the adsorption isotherm data. The results are shown in Figs. 4 and 5, and Table 2.

The T151 sorption isotherms on the penoxsulam surface were consistent with the Langmuir model with  $R^2 > 0.97$  (Table 2). This showed that polyisobutylene succinimide was adsorbed as a single layer on the surface of the penoxsulam within the test concentration range. The quantity of T151 adsorbed on the surfaces of the penoxsulam particles increased from 5.325 to 8.078  $\text{mg}\cdot\text{g}^{-1}$  when the temperature increased from 293.15 to 313.15 K, indicating that the increase in temperature promotes T151 sorption on penoxsulam surfaces.

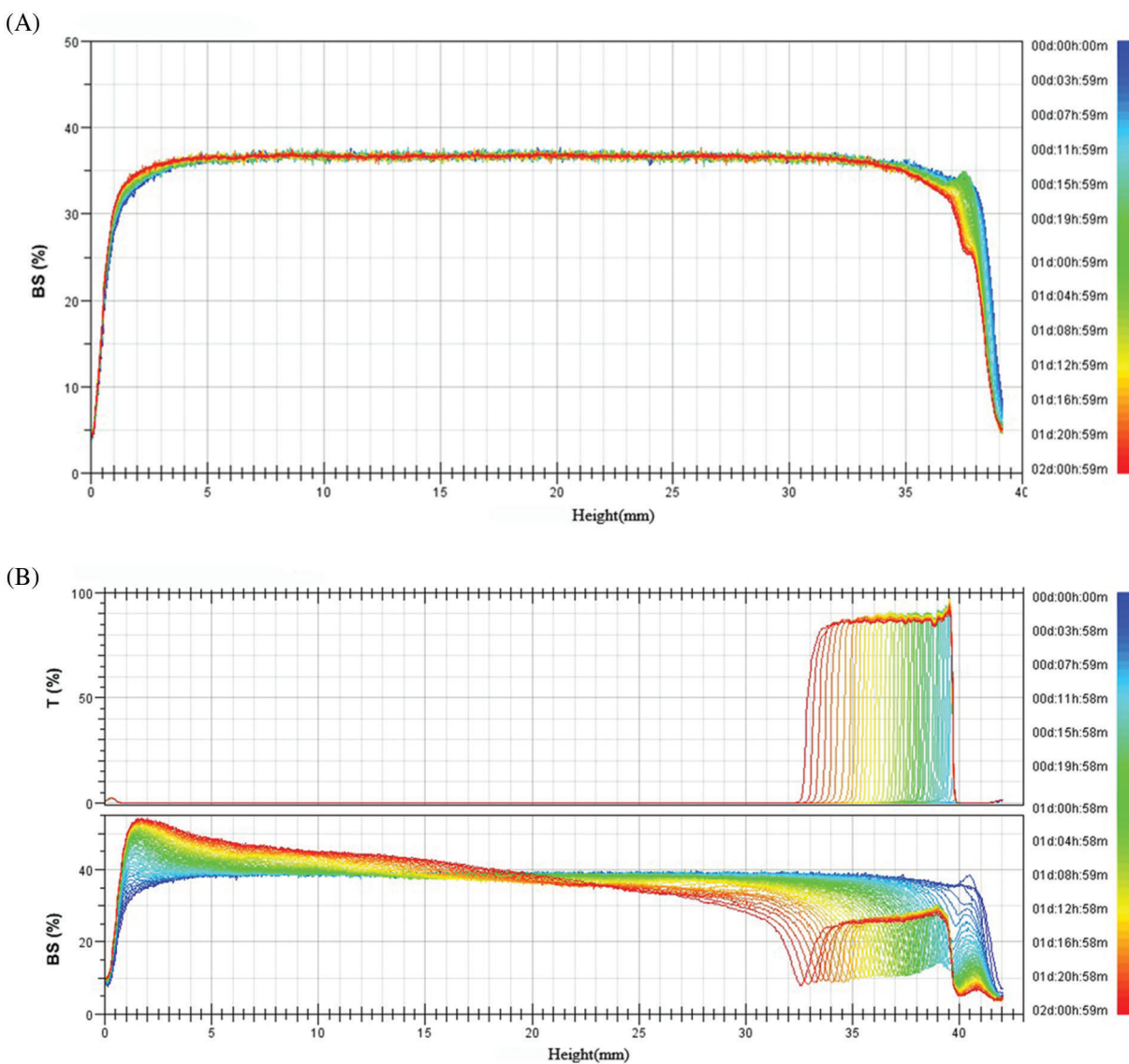


**Figure 2:** Multiple light scattering diagrams of penoxsulam oil dispersible suspension systems. (A) with T151 and (B) without T151

**Table 1:** TSI of penoxsulam oil dispersible suspension systems

| Suspension system | TSI (top) | TSI (middle) | TSI (bottom) | TSI (total) |
|-------------------|-----------|--------------|--------------|-------------|
| with T151         | 0.6       | 0.6          | 0.2          | 1.6         |
| without T151      | 9.9       | 5.5          | 0.9          | 39.0        |

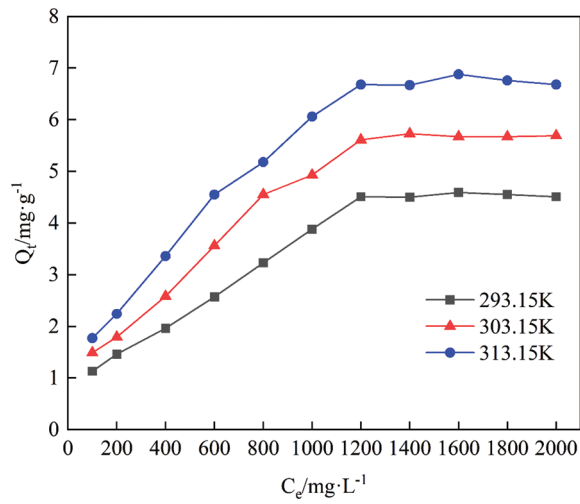


**Figure 3:** Adsorption isotherms of dispersant T151 onto penoxsulam particles at three different temperatures

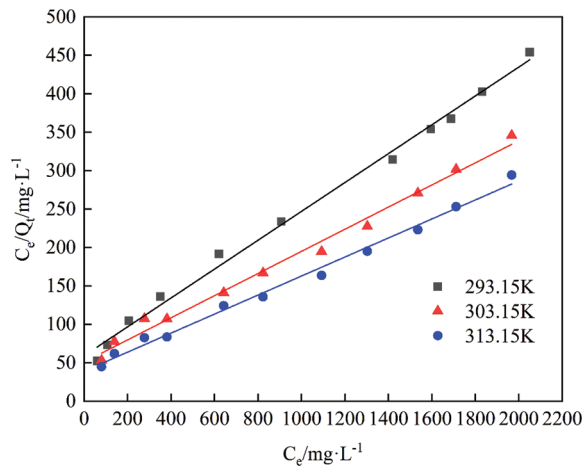


**Figure 4:** Langmuir adsorption isotherms for T151 onto penoxsulam at three different temperatures

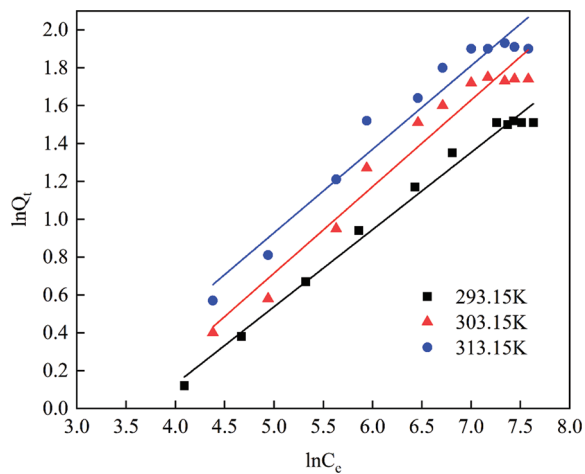


**Figure 5:** Freundlich adsorption isotherms for T151 onto penoxsulam at three different temperatures

**Table 2:** Fitting parameters of Langmuir and Freundlich equations at three temperatures

| T/K    | Fitted by Langmuir equation       |                                 |        | Fitted by Freundlich equation |       |        |
|--------|-----------------------------------|---------------------------------|--------|-------------------------------|-------|--------|
|        | $Q_e/\text{mg}\cdot\text{g}^{-1}$ | $b/\text{L}\cdot\text{mg}^{-1}$ | $R^2$  | $K_f$                         | $n$   | $R^2$  |
| 293.15 | 5.325                             | 0.090                           | 0.9944 | 0.223                         | 2.453 | 0.9887 |
| 303.15 | 6.944                             | 0.136                           | 0.9905 | 0.209                         | 2.191 | 0.9584 |
| 313.15 | 8.078                             | 0.206                           | 0.9924 | 0.280                         | 2.270 | 0.9529 |

### 3.2.3 Thermodynamics Analysis

Research on adsorption thermodynamics includes the examination of the tendency, extent, and driving factors of the sorption process, which is of great significance to analyze the sorption laws, features, and mechanisms. The T151 sorption thermodynamics on the face of the penoxsulam granules were studied by calculating the thermodynamic parameters. The sorption free energy change ( $\Delta G^\theta$ ), sorption enthalpy change ( $\Delta H^\theta$ ), and sorption entropy change ( $\Delta S^\theta$ ) results are shown in Table 3.

**Table 3:** Thermodynamic calculation results

| T/K    | K      | $\Delta G^\theta/\text{kJ}\cdot\text{mol}^{-1}$ | $\Delta H^\theta/\text{kJ}\cdot\text{mol}^{-1}$ | $\Delta S^\theta/\text{J}\cdot\text{mol}^{-1}\cdot\text{K}^{-1}$ |
|--------|--------|---|---|--|
| 293.15 | 3889.3 | -20.15  | 31.59   | 176.50   |
| 303.15 | 5877.2 | -21.87  |   | 176.35   |
| 313.15 | 8902.2 | -23.68  |   | 176.50   |

At different temperatures, the  $\Delta G^\theta$  of T151 on the surface of penoxsulam particles was negative, and its absolute value increased with increasing temperature, indicating that the sorption process could proceed spontaneously and that the adsorption rate increased with increasing temperature. The positive  $\Delta S^\theta$  values at the three temperatures indicate that the T151 adsorption process on the penoxsulam surface was entropy-increasing, suggesting that the dispersion degree of the system was improved, and that the dispersion effect on the penoxsulam particles was greater than the tendency to reduce entropy due to the dispersant adsorption.

The  $\Delta H^\theta$  value was positive, indicating that the adsorption was an endothermic process, and the increase in temperature was beneficial to the adsorption of the T151 dispersant on the surface of the penoxsulam particles. The value of the adsorption enthalpy change indicates the type of adsorption force. The van der Waals force is smaller than  $20 \text{ kJ}\cdot\text{mol}^{-1}$ , the hydrogen bonding force is between  $20\text{--}40 \text{ kJ}\cdot\text{mol}^{-1}$ , and the chemical bonding force is greater than  $60 \text{ kJ}\cdot\text{mol}^{-1}$  [37]. The  $\Delta H^\theta$  value of the T151 dispersant on the surface of the penoxsulam particles was  $31.59 \text{ kJ}\cdot\text{mol}^{-1}$  (Table 3), suggesting that the adsorption process is an endothermic process, is a physical adsorption process, and the main force is hydrogen bonds. The temperature increase promotes the dissociation of hydrogen bonds between the penoxsulam molecules, allowing the dispersant T151 to form a stronger hydrogen bond with penoxsulam and enhance the adsorption. In non-aqueous media, there is no interference from hydrogen ions, which is conducive to hydrogen bond adsorption.

### 3.3 Adsorption Kinetic

#### 3.3.1 Kinetic Curves

In the adsorption kinetics study, the adsorption rate is an important factor that represents how fast the dispersant reaches sorption equilibrium on the pesticide granule surface and determines the dispersing effect of the dispersant to a certain extent. To determine the effect of temperature on the T151 sorption rate on the penoxsulam surface, we measured the relationship between the quantity of T151 on the penoxsulam surface and the adsorption time at the three temperatures.

The amount of T151 adsorbed increased with increasing adsorption time at various temperatures (Fig. 6). The T151 concentration of in the liquor was initially higher than that on the particle surface, thereby rapidly increasing the adsorption rate and the amount of adsorption. During the adsorption process, the T151 concentration on the surface of the penoxsulam particles increased, resulting in a steric hindrance effect, and the sorption rate gradually decreased until equilibrium was reached.

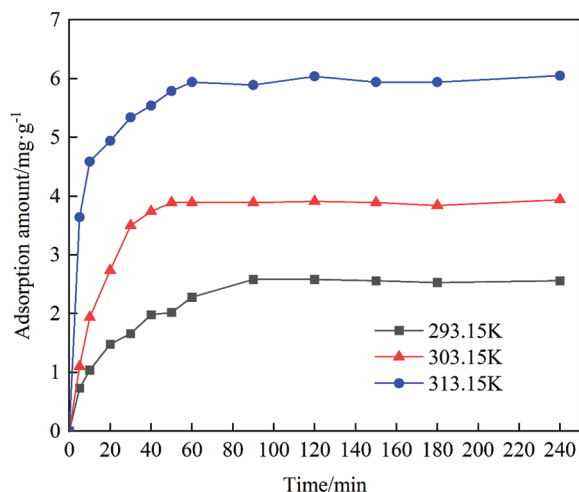


**Figure 6:** Kinetic adsorption isotherms at three different temperatures

#### 3.3.2 Kinetic Models

The T151 sorption process on the penoxsulam surface was studied using pseudo-first-order and pseudo-second-order kinetic models at different temperatures. It was evaluated at a constant adsorption rate.

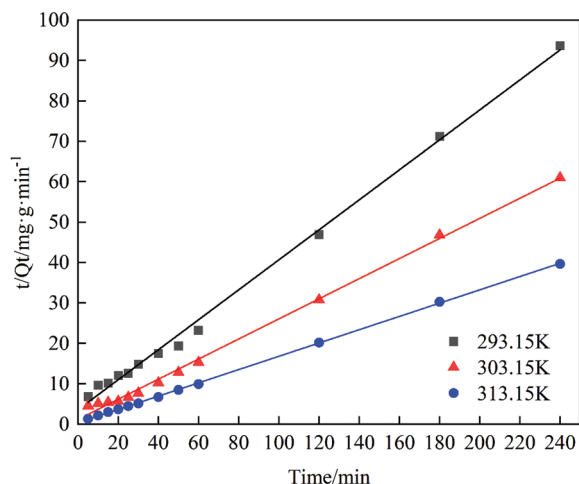


**Figure 7:** Pseudo-second-order adsorption isotherms of dispersant T151 on penoxsulam at three different temperatures

The T151 sorption process on the surface of the penoxsulam granules was most consistent with the pseudo-second-order kinetic adsorption model with  $R^2 > 0.99$  (Fig. 7, Table 4). The pseudo-second-order kinetic model can accurately and comprehensively reflect the entire T151 sorption process. The variation in the adsorption half-life ( $t_{1/2}$ ) at different temperatures indicates that the adsorption equilibrium time decreased and the adsorption rate increased with increasing temperature. This is consistent with the conclusion that the absolute value of the adsorption free energy increases with increasing temperature.

**Table 4:** Fitted values for the kinetic equation at three different temperatures

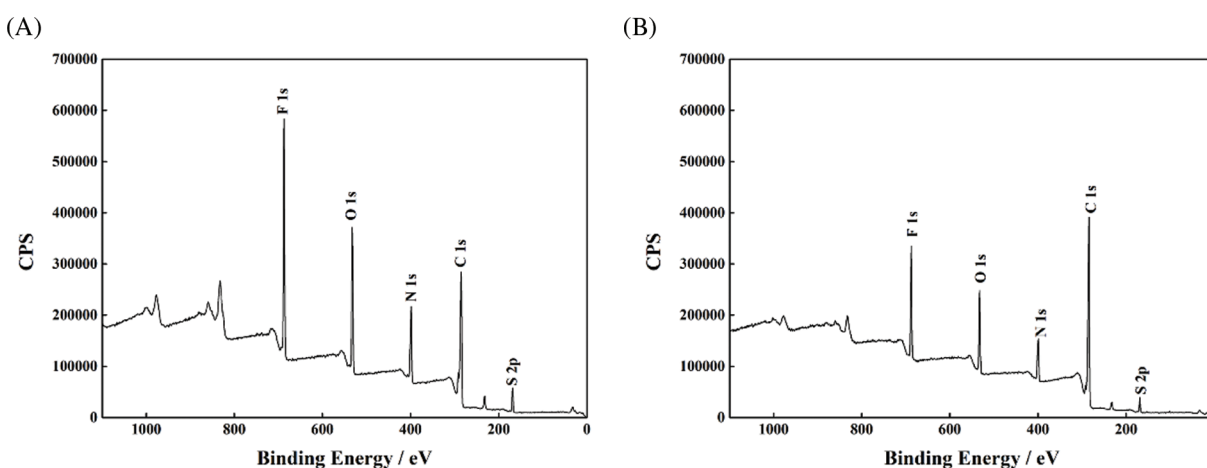
| T/K    | Pseudo-first-order model |   |   |        | Pseudo-second-order model                             |   |   |        |                      |
|--------|--------------------------|---|---|--------|---|---|---|--------|----------------------|
|        | $k_1/\text{min}^{-1}$    | $Q_e \text{ exp}/\text{mg}\cdot\text{g}^{-1}$ | $Q_e \text{ cal}/\text{mg}\cdot\text{g}^{-1}$ | $R^2$  | $k_2/\text{g}\cdot\text{mg}^{-1}\cdot\text{min}^{-1}$ | $Q_e \text{ exp}/\text{mg}\cdot\text{g}^{-1}$ | $Q_e \text{ cal}/\text{mg}\cdot\text{g}^{-1}$ | $R^2$  | $t_{1/2}/\text{min}$ |
| 293.15 | 0.0147                   | 2.607   | 0.647   | 0.4394 | 0.0380  | 2.607   | 2.697   | 0.9967 | 18.24                |
| 303.15 | 0.0108                   | 3.992   | 0.513   | 0.3516 | 0.0503  | 3.992   | 4.032   | 0.9970 | 13.78                |
| 313.15 | 0.0202                   | 6.051   | 0.751   | 0.6053 | 0.0687  | 6.051   | 6.083   | 0.9997 | 10.09                |

An  $E_a$  value of 40–800  $\text{kJ}\cdot\text{mol}^{-1}$  indicates chemical adsorption, and of 5–40  $\text{kJ}\cdot\text{mol}^{-1}$  physical adsorption. The  $E_a$  value calculated using Eq. (10) was 22.57  $\text{kJ}\cdot\text{mol}^{-1}$ . Therefore, according to the thermodynamic analysis, the T151 sorption process on the penoxsulam surface was a physical adsorption process.

### 3.4 Adsorption Layer Thickness

Dispersants can form an adsorbed layer on the surface of solid particles to enhance the stability of a solid-liquid dispersion system. The thickness of the adsorption layer may mirror the steric effect. XPS was used to measure the thickness of the dispersant T151 adsorbed layer on the penoxsulam surface at three different temperatures.

As seen in Figs. 8A and 8B, after the dispersant T151 adsorption, the electron peak strengths of F and S were attenuated, while that of C was notably enhanced. This finding was attributed to the cladding effect of the dispersant, suggesting that T151 formed a fine adsorbed layer on the surface of the penoxsulam particles (Table 5).

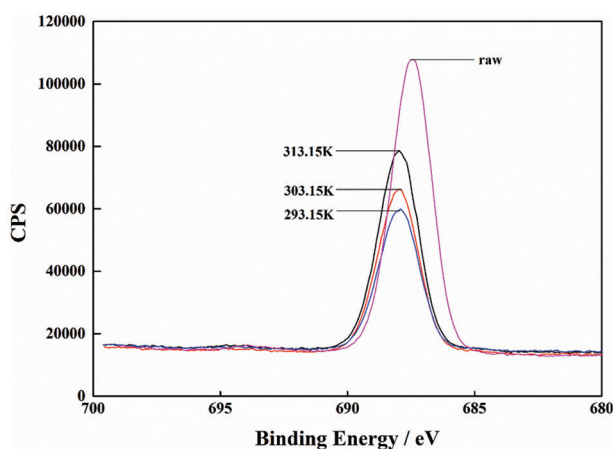


**Figure 8:** XPS results of penoxsulam (A) and adsorbed dispersant T151 (B)

**Table 5:** Concentration of each element and electron bonding energy in penoxsulam with adsorbed T151

| Name    | Penoxsulam  |         | Penoxsulam with T151<br>(293.15 K) |         | Penoxsulam with T151<br>(303.15 K) |         | Penoxsulam with T151<br>(313.15 K) |         |
|---------|-------------|---------|------------------------------------|---------|------------------------------------|---------|------------------------------------|---------|
|         | Position/eV | Conc./% | Position/eV                        | Conc./% | Position/eV                        | Conc./% | Position/eV                        | Conc./% |
| F (1 s) | 687.42      | 33.15   | 687.97                             | 28.26   | 687.97                             | 24.92   | 687.91                             | 22.91   |
| N (1 s) | 398.82      | 12.98   | 399.47                             | 11.95   | 399.27                             | 11.34   | 399.51                             | 10.77   |
| O (1 s) | 533.12      | 22.18   | 533.57                             | 21.15   | 533.57                             | 20.05   | 533.51                             | 19.11   |
| C (1 s) | 285.22      | 28.19   | 284.97                             | 35.34   | 284.87                             | 40.52   | 284.81                             | 44.13   |
| S (2 p) | 168.42      | 3.50    | 168.87                             | 3.31    | 168.97                             | 3.18    | 168.91                             | 3.08    |

Penoxsulam contains F, whereas dispersant T151 does not. Therefore, F was selected as the feature element. By testing the attenuation extent of the F1s photoelectron after passing through the adsorption layer, the mean thickness of the adsorption layer can be obtained (Fig. 9).

**Figure 9:** F (1 s) XPS spectra of penoxsulam surface particles with T151 adsorption dispersant at three different temperatures

Dispersant T151 constituted an adsorbed layer with a certain thickness on the face of the penoxsulam particles. The thicknesses of the adsorbed T151 layers on the penoxsulam surface were 1.582, 2.335, and 3.032 nm at the three temperatures (Table 6). The thickness of the adsorption layer increased with increasing temperature; thus, the increase in temperature was conducive to the sorption of dispersant T151 on the surface of the penoxsulam granules, which is consistent with the sorption isotherm and thermodynamic analysis results.

**Table 6:** Adsorption layer thickness at three different temperatures

| T/K    | d/nm  |
|--------|-------|
| 293.15 | 1.582 |
| 303.15 | 2.335 |
| 313.15 | 3.032 |

### 3.5 Adsorption Morphology and Type

#### 3.5.1 Analysis of Adsorption Morphology

SEM was used to observe the microscopic appearance of the penoxsulam particles before and after the T151 adsorption. As shown in Fig. 10, the penoxsulam surface was smooth before the adsorption of dispersant T151. After the T151 adsorption, minor particles were absorbed onto the surface. Dispersant T151 formed a coating, which can effectively prevent the agglomeration of penoxsulam particles through steric hindrance, thereby improving the physical stability of the penoxsulam oil dispersible suspension.

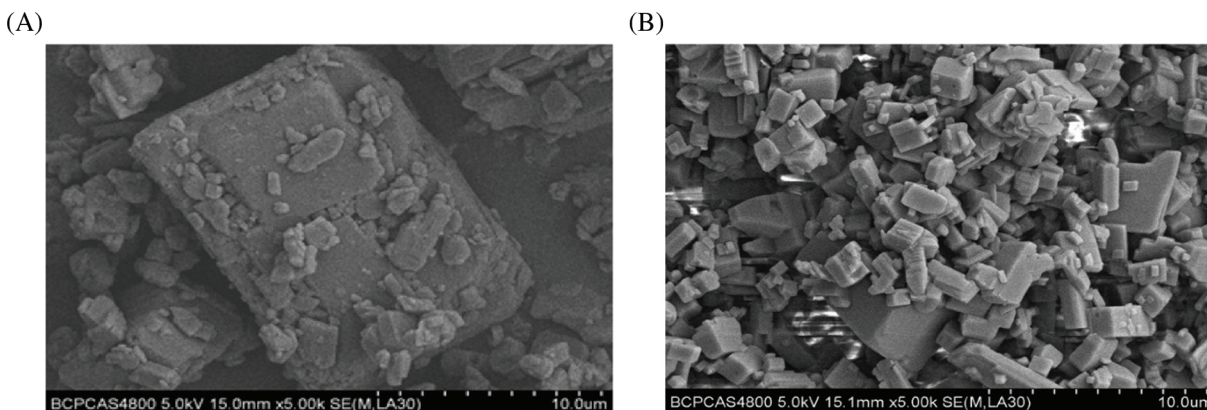


**Figure 10:** SEM images of (A) penoxsulam, (B) penoxsulam + T151

#### 3.5.2 Analysis of Adsorption Type

The T151 adsorption force on the penoxsulam surface was analyzed using FTIR spectroscopy. The FTIR spectra of dispersant T151, penoxsulam, and penoxsulam with adsorbed T151 are shown in Fig. 11.

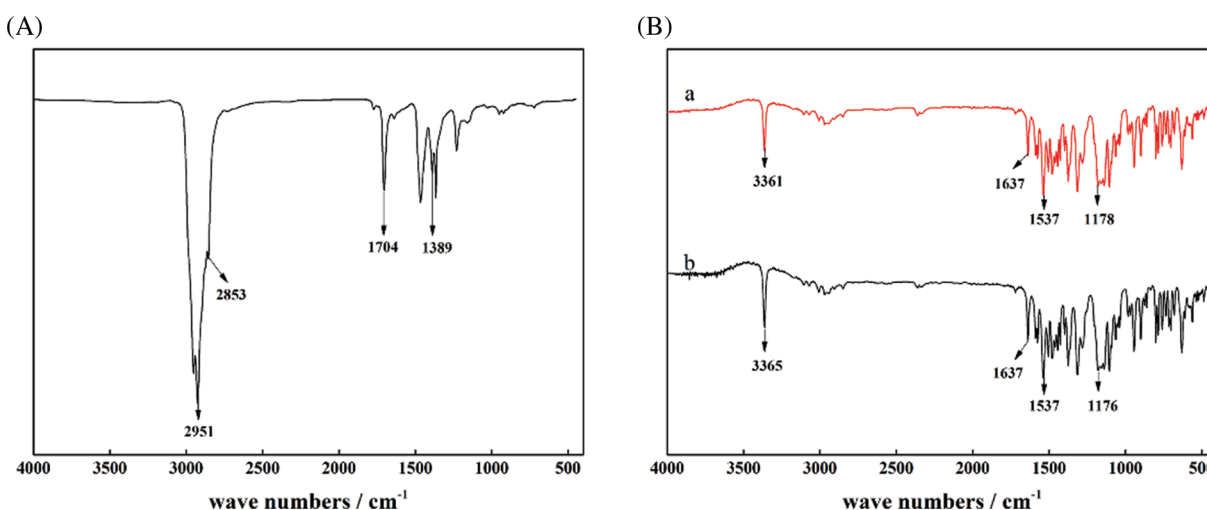


**Figure 11:** FTIR results of dispersant T151. (A) FTIR results of penoxsulam with or without adsorbed T151: (B-a) penoxsulam, (B-b) penoxsulam + T151

The peak at  $2951\text{ cm}^{-1}$  corresponds to the tensile vibrations of C-H,  $-\text{CH}_2$ , and  $-\text{CH}_3$  in the polyisobutylene group. The absorption peak at  $1704\text{ cm}^{-1}$  was the imide group. The C-N tensile vibration absorption peak was at  $1389\text{ cm}^{-1}$  (Fig. 11A).

Compared with that in Fig. 11A, no new absorption peaks appeared after penoxsulam adsorbed dispersant T151 (Fig. 11B), indicating that there was no chemical adsorption between penoxsulam and dispersant T151. After the T151 adsorption, the N-H stretching vibration absorption peak shifted from 3361 to 3365  $\text{cm}^{-1}$ , and the C-F stretching vibration absorption peak shifted from 1178 to 1176  $\text{cm}^{-1}$ . It was shown that there was a hydrogen bond between -F on the surface of the penoxsulam particles and the N-H in dispersant T151, which is the primary force for the sorption of dispersant T151 on the surface of penoxsulam granules.

### 3.5.3 Adsorption Model

Our results indicate that dispersant T151 binds to the surface of penoxsulam particles through polyamine heads in a single-layer multi-point adsorption form, and the primary binding force is hydrogen bonding. Simultaneously, the polyisobutylene chain is hydrophobic, free in a non-aqueous medium, and can form a sorption layer with a certain thickness on the penoxsulam particle surface. Based on these adsorption characteristics, a hypothetical adsorption model of dispersant T151 was proposed (Fig. 12). The adsorption of dispersant T151 on the surface of penoxsulam particles improves the stability of the system through the steric hindrance effect.

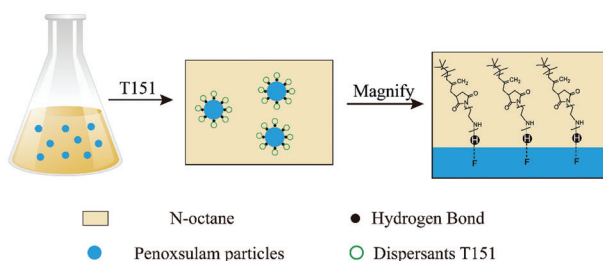


**Figure 12:** Hypothetical model of T151 adsorption onto penoxsulam particle surfaces

## 4 Conclusion

In this study, polyisobutylene succinimide dispersant T151 was shown to improve the stability of a penoxsulam oil dispersible suspension using multiple light scattering techniques. The dispersing effect was exerted by its adsorption on the surface of pesticide particles. Therefore, the adsorption properties of polyisobutylene succinimide dispersant T151 on penoxsulam particles were investigated at the micro level.

The adsorption thermodynamics was comprehensively evaluated. The adsorption isotherm conformed to the Langmuir equation, and the dispersant T151 was adsorbed as a monolayer on the penoxsulam particle surfaces. As the temperature increased, the saturation adsorption capacity increased from 5.325 to 8.078  $\text{mg}\cdot\text{g}^{-1}$ , accompanied by an increase in the adsorption layer thickness from 1.582 to 3.032 nm. Therefore, the increase in temperature is conducive to the sorption of dispersant T151 on the surface of the penoxsulam granules. The thermodynamic parameters  $\Delta G^\theta < 0$ ,  $\Delta H^\theta > 0$ , and  $\Delta S^\theta > 0$  indicate that the dispersant T151 adsorption on the surface of the penoxsulam particles is a spontaneous, endothermic, and entropy-increasing process. The value of  $\Delta H^\theta$  (31.59  $\text{kJ}\cdot\text{mol}^{-1}$ ) indicates that the main sorption force of dispersant T151 on the surface of penoxsulam granules is hydrogen bonding.

The sorption process complied with the pseudo-second-order kinetic model. The adsorption equilibrium time decreased with increasing temperature based on the observation of the adsorption half-life. This indicates that the sorption rate increases with an increase in temperature, which is consistent with the conclusion that the absolute value of the adsorption-free energy increases with an increase in temperature. Moreover, the  $E_a$  value of 22.57  $\text{kJ}\cdot\text{mol}^{-1}$  suggests that the sorption process is a physical adsorption process.

The investigation of the adsorption properties demonstrated that the sorption force is primarily hydrogen bonding, and dispersant T151 maintains its adsorption stability on the surface of penoxsulam particles, thereby improving the stability of the system by the steric hindrance effect. This study provides a significant theoretical basis for the application of polyisobutylene succinimide as a dispersant in oil dispersible systems, sheds light on the innovation and development of oil-dispersible suspensions in the pesticide industry, and addresses the problems that arise during the production, storage, and transportation of oil dispersible suspensions.

**Acknowledgement:** Professor Lixin Zhang provided important support for this research. We would like to thank him for his efforts.

**Funding Statement:** This work was funded by the Foundation (No. LJ2020030) from the Project of the Education Department of Liaoning Province, China.

**Conflicts of Interest:** The authors declare that they have no conflicts of interest regarding this study.

## References

1. Hua, N. Z. (2008). Advance and trend of pesticide formulation development. *Agrochemicals*, 47(2), 79–81+89. <https://doi.org/10.3969/j.issn.1006-0413.2008.02.001>
2. Liao, K., Lu, F., Liu, C. (2015). Application status of oil and ester oil in pesticide products. *Pesticide Science and Administration*, 36(8), 52–57.
3. Tadros, T. F. (2017). Oil-based suspension concentrates. In: *Volume 4 industrial applications II*, pp. 113–130. Germany: De Gruyter.
4. Sekulic, M. T., Boskovic, N., Slavkovic, A., Garunovic, J., Kolakovic, S. et al. (2019). Surface functionalised adsorbent for emerging pharmaceutical removal: Adsorption performance and mechanisms. *Process Safety and Environmental Protection*, 125, 50–63. <https://doi.org/10.1016/j.psep.2019.03.007>
5. Pretti, O. A., Zanin, L. J., Pelinsom, M. J., Lucas, M. S., Silvestre, R. V. G. et al. (2021). A review of pesticides sorption in biochar from maize, rice, and wheat residues: Current status and challenges for soil application. *Journal of Environmental Management*, 300, 113753. <https://doi.org/10.1016/J.JENVMAN.2021.113753>
6. Guo, Z., Gui, Q., Zhang, B., Ren, S., Zhang, S. et al. (2017). Application of polycarboxylate and naphthalenesulfonate dispersants in high concentration suspension concentrate. *Chemical Journal of Chinese Universities*, 38(7), 1278–1285. <https://doi.org/10.7503/cjcu20160848>
7. Wang, S., Yu, S., Feng, J., Liu, S. (2021). Multifunctional lubricant additive derived from polyisobutylene succinimide dispersant. *Journal of Dispersion Science and Technology*, 42(3), 396–406. <https://doi.org/10.1080/01932691.2020.1729172>
8. Chavez-Miyauchi, T. E., Zamudio-Rivera, L. S., Barba-Lopez, V. (2013). Aromatic polyisobutylene succinimides as viscosity reducers with asphaltene dispersion capability for heavy and extra-heavy crude oils. *Energy & Fuels*, 27, 1994–2001. <https://doi.org/10.1021/ef301748n>
9. Pirouz, S., Wang, Y., Chong, J., Duhamel, J. (2015). Chemical modification of polyisobutylene succinimide dispersants and characterization of their associative properties. *Journal of Physical Chemistry B*, 119(37), 12202–12211. <https://doi.org/10.1021/acs.jpcc.5b04515>
10. Shi, X., Cheng, C., Peng, F., Hou, W., Lin, X. et al. (2022). Adsorption properties of graphene materials for pesticides: Structure effect. *Journal of Molecular Liquids*, 364, 119967. <https://doi.org/10.1016/J.MOLLIQ.2022.119967>
11. Reid, J., Barker, J. (2013). Understanding polyisobutylene succinimides (PIBSI) and internal diesel injector deposits. *SAE Technical Papers*. <https://doi.org/10.4271/2013-01-2682>
12. Zhang, M., Li, L., Xu, J., Sun, D. (2013). Effect of polyisobutylene succinimide on low-temperature rheology and dispersibility of clay particles in mineral oil. *Colloids & Surfaces A: Physicochemical & Engineering Aspects*, 431, 133–141. <https://doi.org/10.1016/j.colsurfa.2013.04.034>

13. Xu, Y., Sun, B., Ma, C., Zhang, P., Cai, M. et al. (2011). XPS and SEM analysis of adsorption of hyperdispersant on atrazine particles. *Spectroscopy and Spectral Analysis*, 31(9), 2569–2573. <https://doi.org/10.3964/j.issn.1000-0593.2011.09.058>
14. Xu, Y., Ma, C., Jia, Y., Cai, M., Hu, Y. et al. (2011). Infrared and Raman spectroscopy study on the adsorption of hyperdispersant on atrazine particles. *Spectroscopy and Spectral Analysis*, 31(3), 640–643. [https://doi.org/10.3964/j.issn.1000-0593\(2011\)03-0640-04](https://doi.org/10.3964/j.issn.1000-0593(2011)03-0640-04)
15. Zhang, Z., Lu, F., Chen, T., Liu, Y., Luo, W. (2009). Adsorption properties of styrene acrylic copolymer dispersant at the interface of fluorsin particles. *Chemical Journal of Chinese Universities*, 30(2), 332–336. <https://doi.org/10.3321/j.issn:0251-0790.2009.02.022>
16. Pang, Y., Liu, L., Lou, H., Yi, C., Qiu, X. (2012). Adsorption characteristics of lignosulfonate on the surface of enoylmorpholine particles. *Chemical Journal of Chinese Universities*, 33(8), 1820–1825. <https://doi.org/10.3969/j.issn.0251-0790.2012.08.034>
17. Ma, C., Xu, Y., Guo, X., Luo, X., Wu, X. (2013). Adsorption properties of polycarboxylic acid comb copolymer hyperdispersant at the interface of fipronil particles. *Chemical Journal of Chinese Universities*, 34(6), 1441–1449. <https://doi.org/10.7503/cjcu20121138>
18. Hao, H., Feng, J., Ma, C., Fan, T., Wu, X. (2013). Adsorption thermodynamics and kinetics of three anionic polymeric dispersants onto imidacloprid particle surface. *CIESC Journal*, 64(10), 3838–3850. <https://doi.org/10.3969/j.issn.0438-1157.2013.10.048>
19. Jabusch, T. W., Tjeerdema, R. S. (2005). Partitioning of penoxsulam, a new sulfonamide herbicide. *Journal of Agricultural & Food Chemistry*, 53(18), 7179–7183. <https://doi.org/10.1021/jf050767g>
20. Farooq, M., Hussain, M., Khan, M. B., Shahid, M., Lee, D. J. (2012). Efficient weeds control with penoxsulam application ensures higher productivity and economic returns of direct seeded rice. *International Journal of Agriculture & Biology*, 14(6), 901–907. <https://doi.org/10.1021/jf3034804>
21. Zhang, H., Liu, R., Li, H., Zhou, F. (2021). Purification and separation of astragalosides from astragalus membranaceus hairy roots. *Chemistry of Natural Compounds*, 57(5), 978–981. <https://doi.org/10.1007/S10600-021-03530-8>
22. Wang, L., Gao, C., Feng, J., Xu, Y., Zhang, L. (2020). Adsorption properties of comb-shaped polycarboxylate dispersant onto different crystal pyraclostrobin particle surfaces. *Molecules*, 25(23), 5637. <https://doi.org/10.3390/molecules25235637>
23. Hao, H., Feng, J., Chen, W., Liu, W., Wu, X. (2014). Adsorption characteristics of styrene-sodium methacrylate copolymer on imidacloprid particle surface. *CIESC Journal*, 65(12), 5067–5074. <https://doi.org/10.3969/j.issn.0438-1157.2014.12.057>
24. Hao, H., Ma, C., Feng, J., Fan, T., Chen, B. et al. (2013). Adsorption of polycarboxylate dispersant onto imidacloprid particle surfaces. *CIESC Journal*, 64(8), 2898–2906. <https://doi.org/10.3969/j.issn.0438-1157.2013.08.028>
25. Sun, Y., Deac, A., Zhang, G. (2019). Assessing physical stability of colloidal dispersions using turbiscan optical analyzer. *Molecular Pharmaceutics*, 16(2), 877–885. <https://doi.org/10.1021/acs.molpharmaceut.8b01194>
26. Vall-Llosera, M., Jessen, F., Henriët, P., Marie, R., Casanova, F. (2021). Physical stability and interfacial properties of oil in water emulsion stabilized with pea protein and fish skin gelatin. *Food Biophysics*, 16(1), 139–151. <https://doi.org/10.1007/s11483-020-09655-7>
27. Meng, J., Cui, J., Yu, S., Jiang, H., Zhong, C. et al. (2019). Preparation of aminated chitosan microspheres by one-pot method and their adsorption properties for dye wastewater. *Royal Society Open Science*, 6(5), 182226. <https://doi.org/10.1098/rsos.182226>
28. Costantino, V., Elga, M., Cristiano, C., Arianna, D. B., Alessandra, C. (2020). Adsorption and degradation of three pesticides in a vineyard soil and in an organic biomix. *Environments*, 7(12), 113. <https://doi.org/10.3390/ENVIRONMENTS7120113>
29. Chakraborty, S., Mukherjee, A., Das, S., Maddela, N. R., Iram, S. et al. (2021). Study on isotherm, kinetics, and thermodynamics of adsorption of crystal violet dye by calcium oxide modified fly ash. *Environmental Engineering Research*, 26(1), 210–222. <https://doi.org/10.4491/eer.2019.372>

30. Azizian, S., Eris, S., Wilson, L. D. (2018). Re-evaluation of the century-old langmuir isotherm for modeling adsorption phenomena in solution. *Chemical Physics*, 513, 99–104. <https://doi.org/10.1016/j.chemphys.2018.06.022>
31. Mironyuk, V. N., Al-Alwani, A. J. K., Begletsova, N. N., Gavrikov, M. V., Kolesnikova, A. S. et al. (2021). Study of langmuir monolayers and langmuir-schaefer films based on symmetrical meso-aryl-substituted porphyrin derivative. *Journal of Physics: Conference Series*, 2086(1), 012195. <https://doi.org/10.1088/1742-6596/2086/1/012195>
32. Kang, J., Guo, D. (2022). Exact traveling wave solutions for the system of the ion sound and langmuir waves by using three effective methods. *Results in Physics*, 35, 105390. <https://doi.org/10.1016/J.RINP.2022.105390>
33. Chang, C. K., Tun, H., Chen, C. C. (2020). An activity-based formulation for langmuir adsorption isotherm. *Adsorption-Journal of the International Adsorption Society*, 26(3), 375–386. <https://doi.org/10.1007/s10450-019-00185-4>
34. Lu, L., Na, C. (2022). Gibbsian interpretation of langmuir, freundlich and temkin isotherms for adsorption in solution. *Philosophical Magazine Letters*, 102(7), 239–253. <https://doi.org/10.1080/09500839.2022.2084571>
35. Nuryanti, S., Suherman, Rahmawati, S., Amalia, M., Santoso, T. et al. (2021). Langmuir and Freundlich isotherm equation test on the adsorption process of Cu (II) metal ions by cassava peel waste (*Manihot esculenta crantz*). *Journal of Physics: Conference Series*, 2126(1), 012022. <https://doi.org/10.1088/1742-6596/2126/1/012022>
36. Firdaus, P. M., Wahyuningsih, S., Rahmawati, F., Kusumaningsih, T. (2020). Freundlich adsorption isotherm in the perspective of chemical kinetics (III): Isolation method approach. *IOP Conference Series Materials Science and Engineering*, 858(1), 012010. <https://doi.org/10.1088/1757-899x/858/1/012010>
37. Jagabandhu, R., Kumar, S. S., Tridib, T. (2021). Adsorption of toxic organophosphorus pesticides from aqueous medium using dextrin-graft-poly(2-acrylamido-2-methyl propane sulfonic acid-co-acrylic acid) copolymer: Studies on equilibrium kinetics, isotherms, and thermodynamics of interactions. *Polymer Engineering & Science*, 61(11), 2861–2881. <https://doi.org/10.1002/PEN.25805>
38. Zhao, S., Liu, S., Wang, F., Lu, X., Li, Z. (2021). Sorption behavior of 6:2 chlorinated polyfluorinated ether sulfonate (F-53B) on four kinds of nano-materials. *Science of the Total Environment*, 757, 144064. <https://doi.org/10.1016/j.scitotenv.2020.144064>
39. Mukesh, S., Sujoy, R., Sandhik, R., Pallav, M., Sushovan, D. et al. (2022). Characterization of organophosphate pesticide sorption of potato peel biochar as low cost adsorbent for chlorpyrifos removal. *Chemosphere*, 297, 134112. <https://doi.org/10.1016/J.CHEMOSPHERE.2022.134112>
40. Jie, W., Xue, H., Lin, H., Ying, Z., Wei, C. (2010). A critical study on the adsorption of heterocyclic sulfur and nitrogen compounds by activated carbon: Equilibrium, kinetics and thermodynamics. *Chemical Engineering Journal*, 164(1), 29–36. <https://doi.org/10.1016/j.cej.2010.07.068>
41. Tan, K. L., Hameed, B. H. (2017). Insight into the adsorption kinetics models for the removal of contaminants from aqueous solutions. *Journal of the Taiwan Institute of Chemical Engineers*, 74, 25–48. <https://doi.org/10.1016/j.jtice.2017.01.024>
42. Jafari, S. M., Ganje, M., Dehnad, D., Ghanbari, V., Hajitabar, J. (2017). Arrhenius equation modeling for the shelf life prediction of tomato paste containing a natural preservative. *Journal of Food Agriculture and Environment*, 97(15), 5216–5222. <https://doi.org/10.1002/jsfa.8404>
43. Al-Gaashani, R., Najjar, A., Zakaria, Y., Mansour, S., Atieh, M. A. (2019). XPS and structural studies of high quality graphene oxide and reduced graphene oxide prepared by different chemical oxidation methods. *Ceramics International*, 45(11), 14439–14448. <https://doi.org/10.1016/j.ceramint.2019.04.165>
44. Luo, J., Niu, Q., Jin, M., Cao, Y., Ye, L. et al. (2019). Study on the effects of oxygen-containing functional groups on HgO adsorption in simulated flue gas by XAFS and XPS analysis. *Journal of Hazardous Materials*, 376, 21–28. <https://doi.org/10.1016/j.jhazmat.2019.05.012>
45. Erdem, B., Hunsicker, R. A., Simmons, G. W., Sudol, E. D., Dimonie, V. L. et al. (2001). XPS and FTIR surface characterization of TiO<sub>2</sub> particles used in polymer encapsulation. *Langmuir*, 17(9), 2664–2669. <https://doi.org/10.1021/la0015213>